Presented at the 4th Symposium on the Cerro Prieto Geothermal Field, August 10-12, 1982, Guadalajara, Mexico.

LBL-14652
CP-21

LBL--14652

DE83 009209

SIMULATION AND RESISTIVITY MODELING OF A GEOTHERMAL RESERVOIR WITH WATERS OF DIFFERENT SALINITY

by

K. Pruess, M. Wilt, G.S. Bodvarsson, and N.E. Goldstein

Earth Sciences Division
Lawrence Berkeley Laboratory
University of California
Berkeley, California 94720

October 1982

This work was supported by the Assistant Secretary for Conservation and Renewable Energy, Office of Renewable Technology, Division of Geothermal and Hydropower Technologies of the U.S. Department of Energy under Contract No. DE-AC03-76SF00098.

DISCLAIMER

SIMULATION AND RESISTIVITY MODELING OF A GEOTHERMAL RESERVOIR WITH WATERS OF DIFFERENT SALINITY

by

K. Pruess, M. Wilt, G. S. Bodvarsson, and N. E. Goldstein
Lawrence Berkeley Laboratory, University of California
Berkeley, California 94720

ABSTRACT

Apparent resistivities measured by means of repetitive dipole-dipole surveys show significant changes within the Cerro Prieto reservoir. The changes are attributed to production and natural recharge. To better understand the observed geophysical phenomena, we performed a simple reservoir simulation study combined with the appropriate DC resistivity calculations to determine the expected magnitude of apparent resistivity change. We consider production from a liquid-dominated reservoir with dimensions and parameters of the Cerro Prieto "A" reservoir and assume lateral and vertical recharge of colder and less saline waters. Based on rather schematic one- and two-dimensional reservoir simulations, we calculate changes in formation resistivity which we then transform into changes in apparent resistivity that would be observed at the surface. Simulated changes in apparent resistivities over the production zone show increases of 10 to 20% over a 3 year period at the current rate of fluid extraction. Changes of this magnitude are not only within our ability to discern using proper field techniques, but are consistent in magnitude with some of the observed effects. However, the patterns of apparent resistivity changes in the simulated dipole-dipole pseudosection only partially resemble the observed field data. This is explained by the fact that the actual fluid recharge into the "A" reservoir is more complicated than assumed in our simple, schematic recharge models. DC resistivity monitoring appears capable of providing indirect information on fluid flow processes in a producing geothermal reservoir. Such information is extremely valuable for the development of quantitative predictions of future reservoir performance.

INTRODUCTION

Surface resistivity measurements have often been successfully employed in geothermal exploration because geothermal reservoirs usually have an associated resistivity anomaly which, when interpreted in conjunction with thermal and geochemical data, permits approximate identification of field boundaries. Resistivity data are often relied upon for initial resource evaluation, and for targeting of exploratory wells.

For several years resistivity sounding and modeling have been carried out at Cerro Prieto by the Lawrence Berkeley Laboratory (LBL) and the Comisión Federal de Electricidad (CFE). This work has identified subsurface structures which correlate well with productive horizons and geological models of Cerro Prieto based on independent data. Repetitive resistivity measurements made since 1979 by LBL have achieved a precision and reproducibility which has made it possible to clearly identify temporal changes which can be attributed to the large scale exploitation of the reservoir (Wilt and Goldstein, 1981). It is of interest to note that recent field tests in Utah and Kansas have also shown significant changes in apparent formation resistivity as a consequence of tertiary oil recovery processes (Bartel and Wayland, 1981). Wilt and Goldstein (1981) discuss possible mechanisms which could cause the observed resistivity changes at Cerro Prieto. These include (i) recharge of fluids with different salinity, (ii) formation of two-phase zones near the wells, and (iii) changes in reservoir temperature. The present paper examines in more detail the feasibility of applying resistivity measurements for monitoring reservoir processes caused by exploitation. We apply numerical modeling techniques to study migration of waters of different temperature and salinity in response to production, and we use simulated changes of temperature and salinity to predict changes in apparent resistivity at the surface. Our studies employ rather schematic and simplified reservoir models in order to demonstrate how reservoir engineering and geophysical techniques can be combined for monitoring reservoir processes caused by exploitation. We have not attempted to construct a detailed model of the Cerro Prieto field; however, we have employed formation parameters, thermodynamic conditions, and overall dimensions representative of Cerro Prieto, so that our results should permit a realistic assessment of the proposed methodology.

SIMULATION OF A RESERVOIR WITH TWO WATERS OF DIFFERENT SALINITY

We consider production of liquid water from a porous reservoir with an initial temperature of $T = 300^{\circ}C$. The vertical pressure profile is assumed hydrostatic, with an average pressure $P_{av} = 120$ bars. The reservoir communicates with recharge waters of $T = 100^{\circ}C$ above and/or at the margins. The mass fraction of recharge water is denoted by x; initially $x = 0$ in the reservoir. The recharge waters are assumed to have different (lower) salinity than the water initially in place in the reservoir. For purposes of numerical modeling, however, we ignore all differences in thermophysical properties arising from different salinity, such as differences in

viscosity, density, boiling curve, etc. We write separate mass balances for "water 1" (x = 0) and "water 2" (x = 1), which makes it possible to keep track of the individual waters as they start flowing and mixing in response to production. A similar approach was presented by Geshelin et al. (1981) for tracing fluid migration during steam assisted oil recovery.

The reservoir simulations reported below were carried out with LBL's compositional simulator MULKOM, which is similar to the geothermal reservoir simulator SHAFT79 (Pruess and Schroeder, 1980), except that two water components are included. To demonstrate the mixing effects, we present results for two one-dimensional models. We consider a 1-m thick vertical slice of 700-m length and 400-m height, which roughly corresponds to a vertical section from the center of Cerro Prieto A (or upper) reservoir to the margin of the present well field (see Figure 1). The section shown in Figure 1 is produced uniformly at a volumetric rate equal to the actual average rate over the last several years. Assuming reservoir parameters of thickness H = 400 m, radius R = 700 m for the presently exploited portion of Cerro Prieto field, the average production rate of 600 kg/s (=2,160 tons/hr) corresponds to a volumetric rate of 9.74×10^{-7} kg/s.m^3. The total production rate from the 400 x 700 x 1 m^3 section is then 0.273 kg/s. Other model parameters were chosen to represent best estimates for Cerro Prieto reservoir (see Table 1).

In case (a) we study lateral recharge. The top and bottom boundaries are assumed "no flow", whereas conditions of T = 100°C, p = 120 bars, x = 1 are maintained at the right boundary. The left boundary corresponds to the center of the reservoir and is always "no flow" due to symmetry. Thus, the system starts out with a step change in temperature and water composition at the right boundary. For the numerical simulation the reservoir is subdivided into 20 volume elements of 35 m length each. Five sinks with a strength of 0.0546 kg/s each were placed into elements 1, 5, 9, 13, and 17 to approximate a uniform depletion (Figure 1). In response to production, water with T = 100°C, x = 1 starts to invade the reservoir from the margins. The temperature and composition profiles after t = 3 years are shown in Figure 2. The thermal front advances at approximately one fourth the speed of the compositional front, due to heat transfer from the rocks to the cold recharge waters. For the conditions assumed in our modeling study, no two-phase zones form in the reservoir. It should be stressed that the smearing of compositional and thermal fronts is entirely due to numerical dispersion, as our model does not include actual physical dispersion due to multiple flow paths and other mechanisms. For comparison a calculation with a four times finer grid, using 80 grid blocks for the 700 m length is also shown in Figure 2. A much steeper, less dispersed profile is then obtained for the fronts.

Case (b) differs from (a) in that vertical recharge from the top is considered. Before simulating production, we perform gravitational equilibration, keeping p = 120 bars fixed at an elevation of 200 m above reservoir bottom. In the production simulation, the pressure is then maintained at its equilibrium value p = 106.7 bars at the top of the reservoir.

Case (c) is the most realistic of the models considered here. The model is two-dimensional, and deals with both vertical and lateral recharge and gradational changes in temperature and salinity. The vertical recharge zone begins 600 m below ground surface and extends to the reservoir top at 800 m depth (see Figure 3). The reservoir height is again H = 400 m, but the lateral dimension is slightly increased to 1600 m, as compared to 1400 m in the one-dimensional models. Due to symmetry, only one half of the system needs to be modeled. Laterally, the reservoir is connected to a recharge zone of 1000 m length with boundary conditions of T = 100°C, x = 1 on the outer boundary. The initial variations in temperature and fluid composition between reservoir and vertical and lateral recharge boundaries are assumed to be smooth. The following parameterization was used:

(i) composition:

$$x_{in} = \begin{cases} 0 \text{ in reservoir;} \\ f(\ell) \text{ between reservoir and recharge boundary;} \\ 1 \text{ at recharge boundary;} \end{cases}$$

(ii) temperature:

$$T_{in} = \begin{cases} 300°C \text{ in reservoir;} \\ 300 - f(\ell) \times (300-100)°C \text{ between reservoir and recharge boundary;} \\ 100°C \text{ at recharge boundary.} \end{cases}$$

Here ℓ is the distance from the vertical or lateral reservoir boundary, and

$$f(\ell) = \begin{cases} \frac{2}{L^2}\ell^2 & \text{for } \ell < L/2 \\ 1 - \frac{2}{L^2}(\ell - L)^2 & \text{for } \ell > L/2, \end{cases}$$

L is the vertical or lateral distance between reservoir and recharge boundaries ($L_{vertical}$ = 200 m; $L_{lateral}$ = 1000 m).

The computational mesh employs 100 m horizontal and 50 m vertical spacing, for a total of (18 x 8) + (8 x 4) = 176 elements, plus elements for representing the boundaries. The problem is initialized with approximate gravitational equilibrium relative to a reference pressure of p = 120 bars at 1000 m depth. (Due to the temperature differences between reservoir and recharge waters no rigorous gravitational equilibrium is possible). The same volumetric production rate as was used in the one-dimensional models is

employed. Production is divided among four sources, placed in elements D1, E3, D5, and E7 (see Figure 3).

Horizontal permeability is taken to be 100 x 10^{-15} m^2, corresponding to a kH = 40 x 10^{-12} m^3. This agrees closely with the "field value" 36 x 10^{-12} m^3, which can be derived from an average transmissivity kH/μ = 0.4 x 10^{-6} m^3/Pa.s (Liguori, 1979) and μ (300°C) = 9.01 x 10^{-5} Pa.s. Vertical permeability was assumed one tenth of horizontal permeability. For these permeabilities, the reservoir can easily sustain the applied production rate. The largest observed pressure decline after 5 years is approximately 1 MPa, so that pressures remain well above saturation pressure and no two-phase zones evolve.

Temperature profiles for layers C, E, and G after 3 years of simulation are presented in Figure 4. The initial temperature distribution (t = 0) is also plotted for comparison. The figure shows a significant migration (vertical and lateral) of colder waters into the production zone (0-800 meters away from the symmetry line) due to the massive exploitation. The migration of the colder recharge waters from above is evident from the lower temperatures in the G layer in comparison with the temperature profile in the C layer in the production region. Lateral migration of the recharge waters is also evident in Figure 4 when the temperature profiles for layers C and G are compared to the initial temperature distribution (t = 0). The temperatures in layer G are everywhere higher than the temperatures in layers C and E in the outside region (> 800 meters away from the symmetry line) because of bouyancy effects.

The composition profiles for layers C, E, and G after 3 years of simulation are shown in Figure 5. Again the initial composition profile (t = 0) is included for reference. The effects of vertical and lateral recharge, as well as buoyancy effects, are clearly evident. The interior of the production region (left portion of Figure 5) is dominated by vertical recharge, which is strongest for the topmost layer. Accordingly, the mass fraction of recharge water is greatest in layer G, and smallest in layer C near the bottom of the reservoir. A different picture is observed at the reservoir margins at a distance of 800 m from the symmetry line. There lateral recharge is dominant, which, due to buoyancy effects, tends to be stronger in the lower portions of the reservoir, so that x (layer C) > x (layer E) > x (layer G). The buoyancy effects cause x (layer G) to decrease more rapidly away from the lateral recharge boundary (at 1800 m distance from the symmetry line) than is observed for layer E or C. The decrease in x (layer G) is reversed inside the reservoir due to vertical recharge, giving rise to a minimum in x (layer G) near the reservoir margin (800 m). A complex interplay of vertical and lateral recharge is also observed for layer E.

RESISTIVITY MODELING OF A RESERVOIR WITH WATER MIXING

A two dimensional finite difference computer code was used in numerical calculations for resistivity models in this study. The code RESIS2D solves finite difference equations for the electric potentials in or on the surface of a two dimensional half space with an arbitrary conductivity distribution (Dey and Morrison, 1976; Dey, 1976). Computer simulation may be done for a wide variety of surface and downhole resistivity arrays. The accuracy of the code has been verified by comparing results to analytical solutions and analog models.

The code utilizes a mesh of 113 x 16 nodes of which 58 x 13 can be used for arbitrary resistivity distributions. This limited size mesh has posed problems for this study because it is unable to provide fine resolution in the region where the resistivity changes are large. Because of the limited mesh size, only 32 elements can be used to describe resistivity within the production zone, and thus resistivity variations due to temperature and salinity changes were averaged over fairly large cross-sectional areas.

CALCULATION OF RESISTIVITY VARIATIONS

A study of the variations in resistivity due to changes in fluid properties in geothermal systems has recently been published (Ershagi et al., 1981). In the present paper we use those results to calculate resistivity as a function of salinity and temperature.

Figure 6 indicates the effect of salinity and temperature on resistivity for "typical" sediments in a geothermal environment. For our study we assume that recharge waters have .3% dissolved solids by weight and are at a temperature of 100°C. In the production zone the parameters are 1.5% and 300°C, respectively. These values are based on observed water chemistry at Cerro Prieto (Grant et al., 1981). Figure 6 shows that resistivity variations due to salinity and temperature changes can be quite large. In the recharge zone, initial resistivity is 50 percent larger than in the production zone due to temperature variation and more than 300 percent larger due to salinity differences.

The initial subsurface resistivity distribution assumed in this study is shown in Figure 7. The 5 ohm-m surface corresponds to a caprock. The 15.6 ohm-m background is sedimentary rock with 15 percent porosity and saturated with 100°C water at .3 weight percent NaCl. The 15.6 ohm-m resistivity value for the background was calculated from Archie's law. The geothermal reservoir is represented by a 1600 m x 400 m zone buried at a depth of 800 meters. Within the reservoir region the resistivity is initially 2.15 ohm-m. This number was derived by adjusting the background of 15.6 ohm-m for increased salinity and temperature in the reservoir region.

RESULTS OF SAMPLE CALCULATIONS

Resistivity calculations for the three reservoir models presented above were done for the dipole-dipole resistivity array over the producing zone. The calculations assume a station spacing of 800 meters and "n-spacings" of 1 to 8, i.e., the distance between transmitter and receiver is one to eight times the 800 m station spacing. This corresponds to a maximum source-receiver separation of 7200 meters. For the three cases studied (see above), we calculate resistivity pseudosections for dipole-dipole surveys before exploitation and then at times of 0.5, 1, 3, and 5 years after production began. The resistivity distribution is adjusted to account for subsurface temperature and salinity changes due to production. Apparent resistivity differences between the pre-production and subsequent "surveys" are then calculated on a point-by-point basis and presented in pseudo-section form.

Case a - Lateral Recharge

In Figure 8 percent difference pseudosection plots for 1, 3, and 5 years after production begins are given for the lateral recharge case. The plots show a recognizable pattern of change at 1 year which grows increasingly stronger with time. The patterns are similar at all times. The plots show a narrow arcuate band where the effect is largest below which is a "shadow zone" where little effect is observed. The band of maximum change is strongly influenced by current paths that travel through the reservoir region whereas the "shadow zone" represents paths that are only weakly influenced by the reservoir. For all plots, significant apparent resistivity differences are observed at $n = 2$ to $n = 8$ for points directly above the reservoir region.

After 3 years even the central nodes in the production region are affected by the intrusion of colder and less saline water, and resistivity in this region increases sharply. The percent difference pseudosection plot reflects this change by showing a more pronounced apparent resistivity increase in the center of the arc and a reduction of the shadow zone beneath the arc.

Assuming an average survey error of 1-2 percent, which is typical for the Cerro Prieto monitoring studies (Wilt and Goldstein, 1982), it should be possible to detect changes after one year and to quantitatively model data after 2 or 3 years.

Case b - Vertical Recharge

For this case cold water recharge is constrained to flow vertically downward into the reservoir. Figure 9 shows percent difference pseudosections for 1, 3, and 5 years after production begins. The difference pattern is quite similar to the lateral case, an arcuate or chevron pattern with a shadow zone beneath, but in this case the arc is narrower and thicker at the top.

One year resistivity changes are larger than for the lateral case and appear shallower with some significant change even at $n = 1$. After one year the effect is greater than seven percent for a number of points, which is well above the measurement error levels. After five years the pattern appears similar to the lateral case for the same time period.

Case c - Vertical and Lateral Recharge

This case assumes both vertical and lateral recharge, with gradational initial variations in temperature and salinity outside of the production zone. In Figure 10, percent difference pseudo-sections are shown for 0.5, 1, 3, and 5 years after the onset of production. There is very little change after 6 months, and after one year only moderate change is observed. The intermediate zone seems to act as a buffer, slowing the rate of apparent resistivity change compared to the previous cases with step changes in temperature and salinity. After three years much of the less saline water reaches the production region, resulting in rather large resistivity changes. The patterns also seem broader than either the lateral or vertical case with significantly larger magnitudes. After 5 years the maximum resistivity change approaches 25 percent and a change of more than 10 percent occurs for the $n = 1$ points overlying the reservoir. It appears that, due to the smooth spatial variations in temperature and salinity, early time resistivity changes are smaller and late time changes larger than predicted from the one-dimensional step change models (a) and (b).

DISCUSSION

Case (c), the most realistic of the cases studied, has significant implications for resistivity monitoring studies. Despite the large rate of production the apparent resistivity changes are small after one year of production and during such early times reservoir-related changes could be totally obscured by seasonal variations in rainfall, runoff or irrigation (Wilt and Goldstein, 1982). However, given sufficient production time, the recharge waters will affect the reservoir region so that the pattern of resistivity change may help determine the parameters of fluid circulation.

It is interesting to compare our calculated resistivity results to the actual monitoring measurements in Cerro Prieto (Wilt and Goldstein, 1982). Figure 11 shows the percent changes in apparent resistivity along a line over the production region (line E-E') at times of 1, 1.5, and 2.5 years after the 1979 baseline measurements. Additional details concerning the monitoring work are given in Wilt and Goldstein (1982). The field data show a far more complex pattern of change than the relatively simple models used in the present study, but there are some striking similarities in pattern and magnitude of resistivity change, particularly in the production zone which is located between kilometers 9 and 13. This area has shown a continuous and steady

resistivity increase very similar in character to the arc-like patterns of generic model (c) but with only half of the arc present. The other half is replaced with a zone of decreasing resistivity. The pattern seems to suggest that resistivity in the western part of the reservoir may be changing in accordance with our model, but in the eastern portion of the reservoir more complex processes are taking place. According to a fluid flow model, based on a lithofacies analysis and temperature profiles (Halfman et al., 1982), recharge to the "A" reservoir is in part hot water ascending from below and from the east along permeable paths provided by a combination of faults and sandstone units. This circulation system might explain the differences between the actual resistivity changes and those simulated. The obvious next step is to attempt verification of the proposed fluid flow model by means of a more rigorous simulation study.

CONCLUSIONS

A methodology has been presented for indirect study of a geothermal reservoir which combines numerical reservoir simulation with modeling of apparent resistivities as measured with the dipole-dipole technique. For a Cerro Prieto-type reservoir, temporal changes in apparent resistivity due to production and recharge of colder and less saline waters are both calculated and are observed to be substantial over time intervals of several years. It therefore appears feasible to use resistivity surveys as a means for monitoring reservoir processes. While our schematic models predict resistivity changes which are roughly consistent with field observations, more detailed reservoir models are required to adequately represent the field data.

For most geothermal reservoirs, the patterns of fluid flow and resistivity change will be three-dimensional. Therefore, accurate resistivity monitoring requires measurements along several intersecting profiles.

The proposed methodology should also be applicable for monitoring the migration of reinjected fluids.

ACKNOWLEDGEMENT

We thank Drs. M. Lippmann and C.F. Tsang for a critical review of the manuscript. This work was supported by the Assistant Secretary for Conservation and Renewable Energy, Office of Renewable Technology, Division of Geothermal and Hydropower Technologies of the U.S. Department of Energy under Contract No. DE-AC03-76SF00098.

REFERENCES

Bartel, L. C., and J. R. Wayland, 1981. Results from Using the CSAMT Geophysical Technique to Map Oil Recovery Processes. Paper SPE 10230, presented at the 56th Annual Fall Technical Conference and Exhibition of the SPE, San Antonio, Texas, October 5-7, 1981.

Dey, A., 1976. Resistivity Modelling for Arbitrarily Shaped Two Dimensional Structures Part II. Guide to the FORTRAN Algorithm RESIS2D. Lawrence Berkeley Laboratory Report LBL-5283.

Dey, A., and H. F. Morrison, 1976. Resistivity Modelling for Arbitrarily Shaped Two Dimensional Structures Part I. Theoretical Formulation. Lawrence Berkeley Laboratory Report LBL-5233.

Ershaghi, I., E. E. Dougherty, and L. Hardy, 1981. Formation Evaluation in Liquid Dominated Geothermal Reservoirs. Report for Department of Energy No. DOE/ET/28384-T1.

Geshelin, B. M., J. W. Grabowski, and E. C. Pease, 1981. Numerical Study of Transport of Injected and Reservoir Water in Fractured Reservoirs During Steam Stimulation. Paper SPE 10322, presented at 56th Annual Fall Technical Conference and Exhibition of the SPE, San Antonio, Texas, October 5-7, 1981.

Grant, M.A., A. H. Truesdell, and A. Manon M., 1981. Production induced Boiling and Cold Water Entry in the Cerro Prieto Geothermal Reservoir indicated by Chemical and Physical Measurements, in Proceedings, Third Symposium on the Cerro Prieto Geothermal Field, Baja California, Mexico, Lawrence Berkeley Laboratory Report LBL-11967, pp 221-237.

Halfman, S.E., Lippmann, M.J., Zelwer, R., and Howard, J.H., 1982. Fluid Flow Model of the Cerro Prieto Geothermal Field Based on Well Log Interpretation. Lawrence Berkeley Laboratory, LBL-14898, 13 p. (and in Proceedings, Fourth Symposium on the Cerro Prieto Geothermal Field, this volume).

Liguori, P. E., 1979. Simulation of the Cerro Prieto Geothermal Field Using a Mathematical Model, in Proceedings, Second Symposium on the Cerro Prieto Geothermal Field, Mexicali, Baja California, October 17-19, 1979, pp 521-524.

Pruess, K., and R. C. Schroeder, 1980. SHAFT79 User's Manual. Lawrence Berkeley Laboratory Report LBL-10861, Berkeley, California, March 1980.

Wilt, M. J., and N. E. Goldstein, 1981. Results from Two Years of Resistivity Monitoring at Cerro Prieto, in Proceedings, Third Symposium on the Cerro Prieto Geothermal Field, Baja California, Mexico, Lawrence Berkeley Laboratory Report LBL-11967, pp 372-379.

Wilt, M. J., and N. E. Goldstein, 1982. Interpretation of Dipole-Dipole Resistivity Monitoring Data at Cerro Prieto, in Proceedings, Fourth Symposium on the Cerro Prieto Geothermal Field, this volume.

TABLE 1

Parameters for Production Simulation

rock density	2600 kg/m^3
porosity	15%
horizontal permeability	100×10^{-15} m^2
vertical permeability	10×10^{-15} m^2
heat conductivity	2.1 W/m^oC
rock specific heat	900 J/kg^oC
vertical extent of reservoir	400 m
volumetric rate of production	9.74×10^{-7} $kg/s.m^3$
initial reservoir temperature	300°C
average initial reservoir pressure	12 MPa (120 bars)

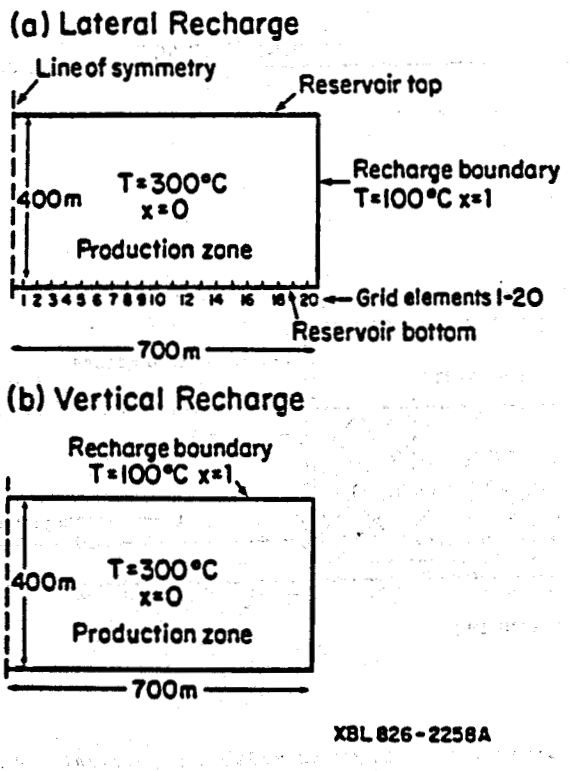

Figure 1. One-dimensional reservoir models for lateral or vertical recharge.

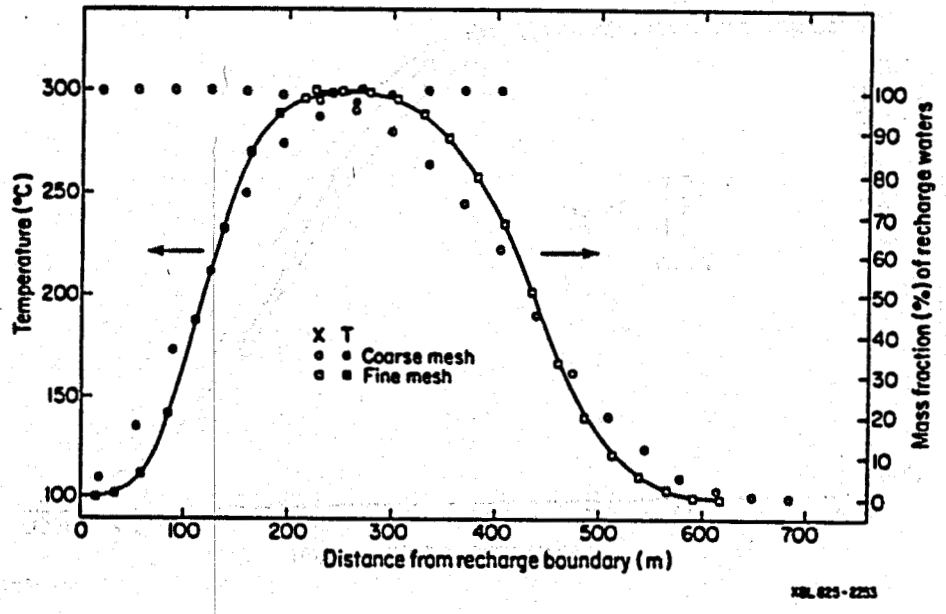

Figure 2. Temperature and composition profiles for lateral recharge after 3 years of production.

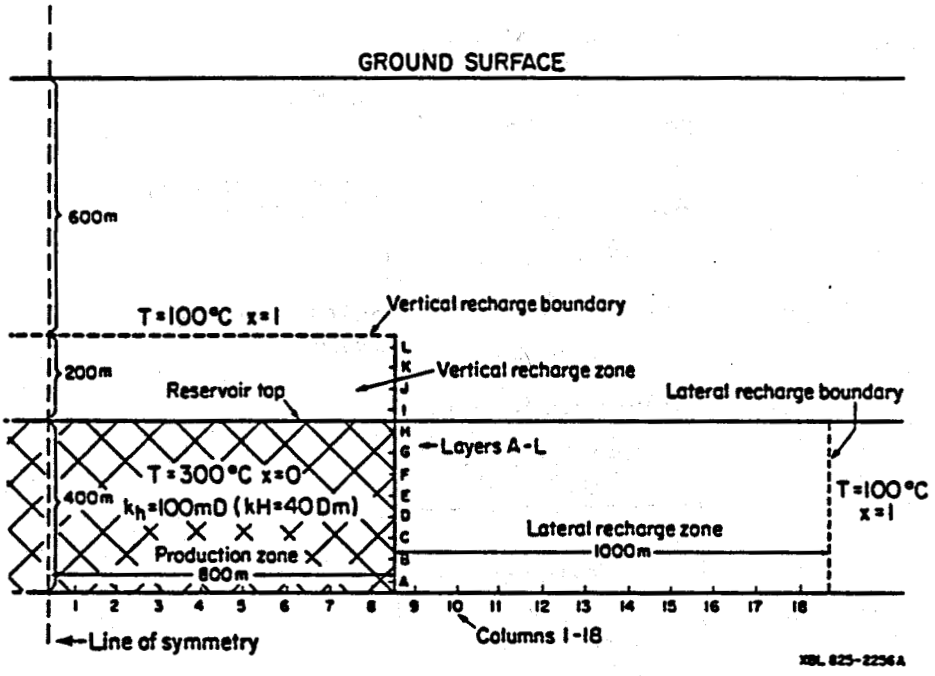

Figure 3. Two-dimensional reservoir model for vertical and lateral recharge.

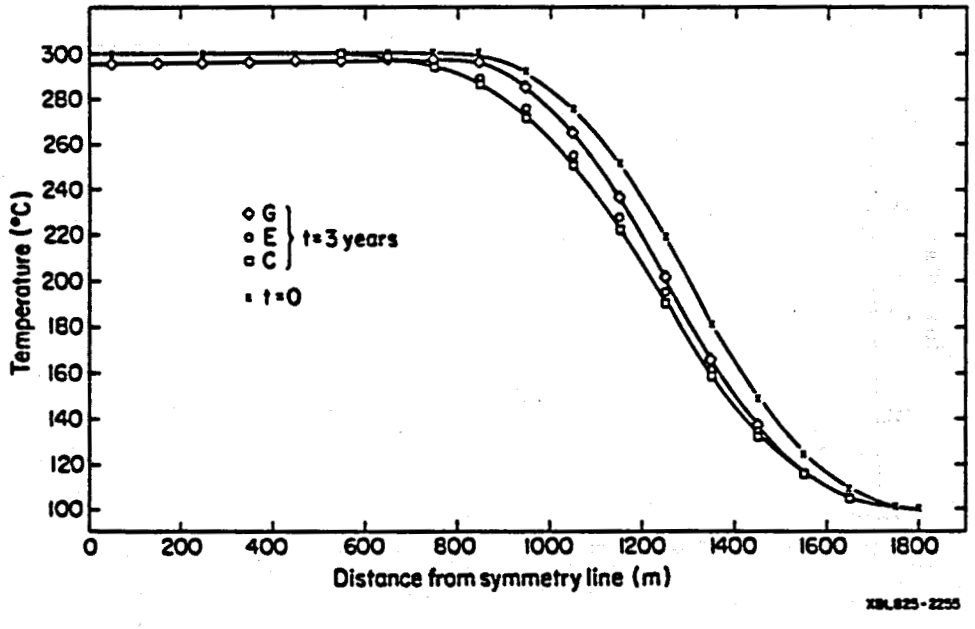

Figure 4. Temperature profiles for two-dimensional model.

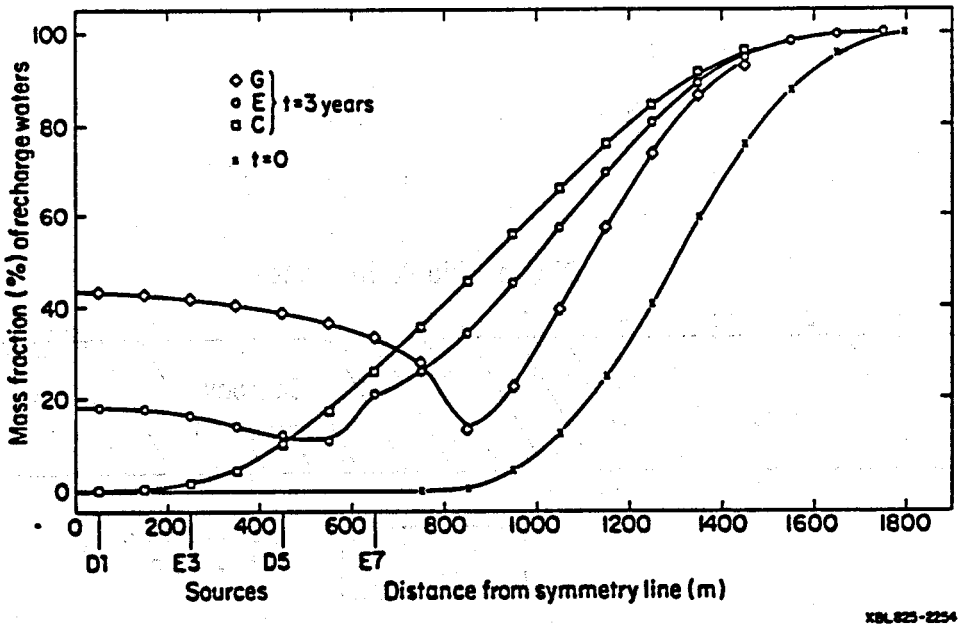

Figure 5. Composition profiles for two-dimensional model.

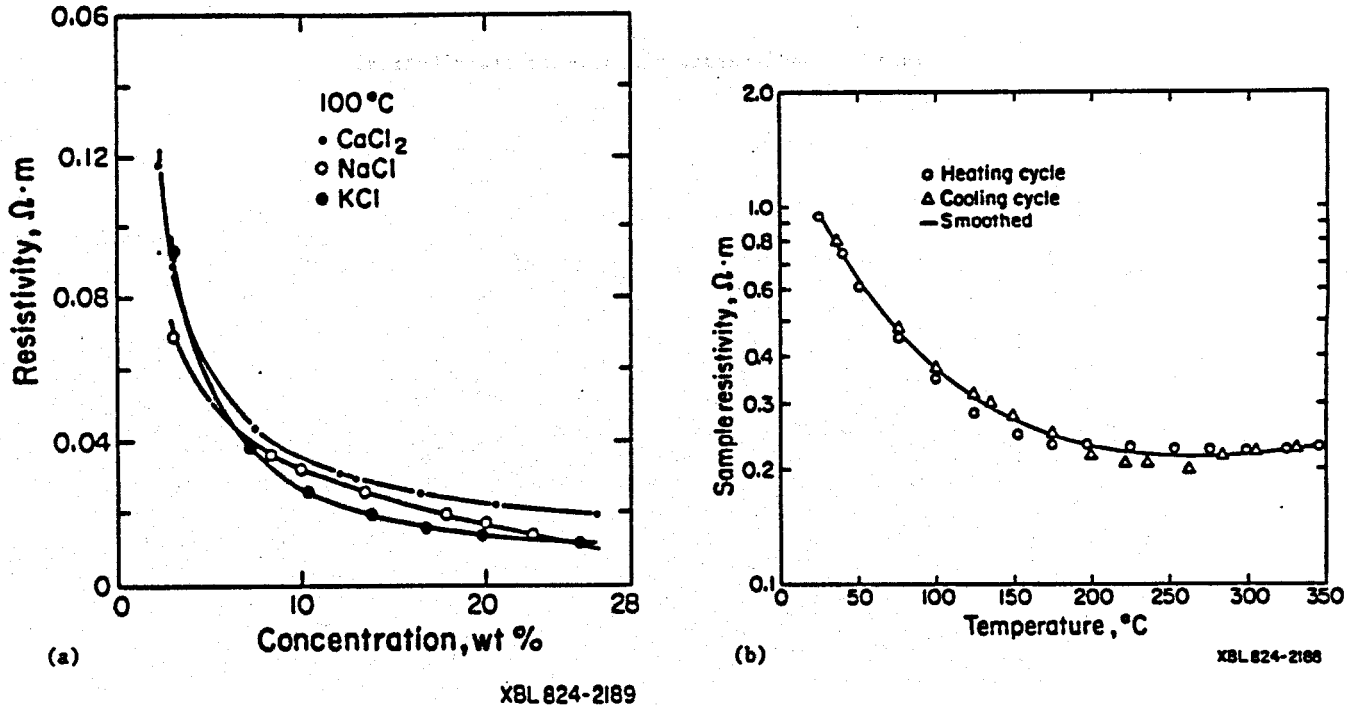

Figure 6. Dependence of resistivity on (a) salinity and (b) temperature for sedimentary rocks.

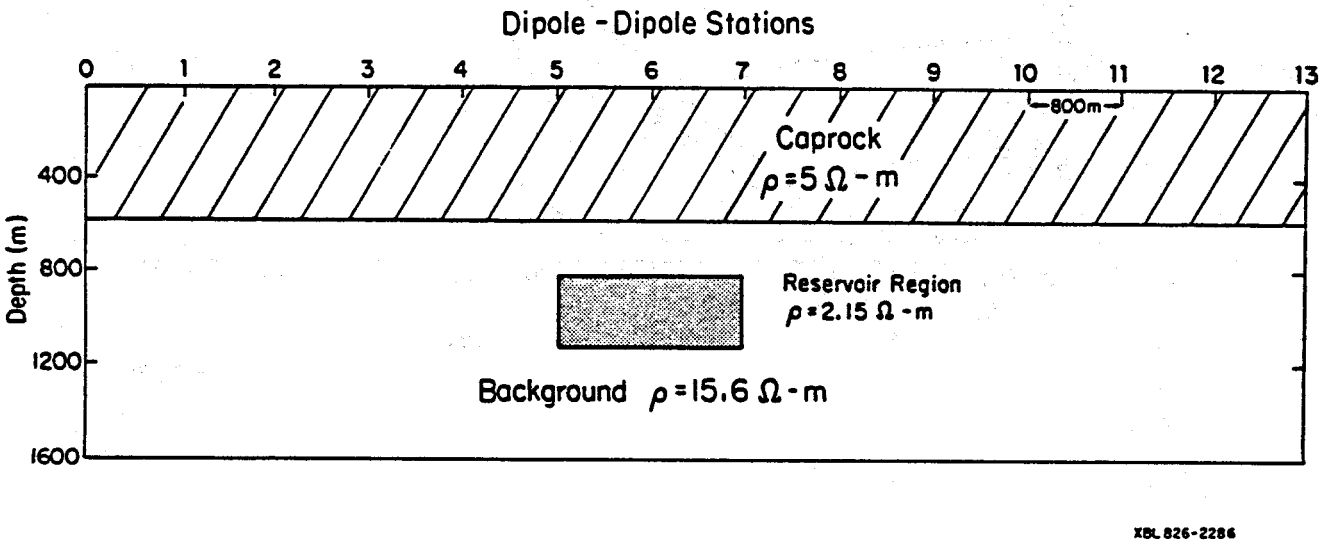

Figure 7. Undisturbed resistivity distribution.

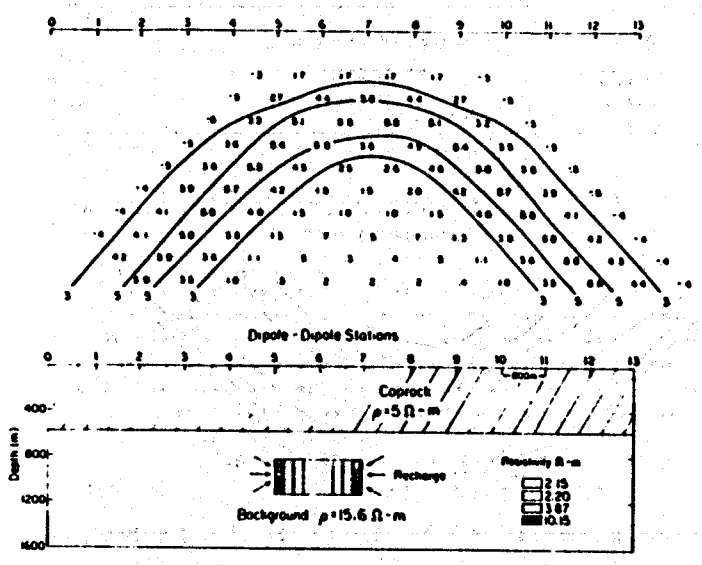

(a) 1 year

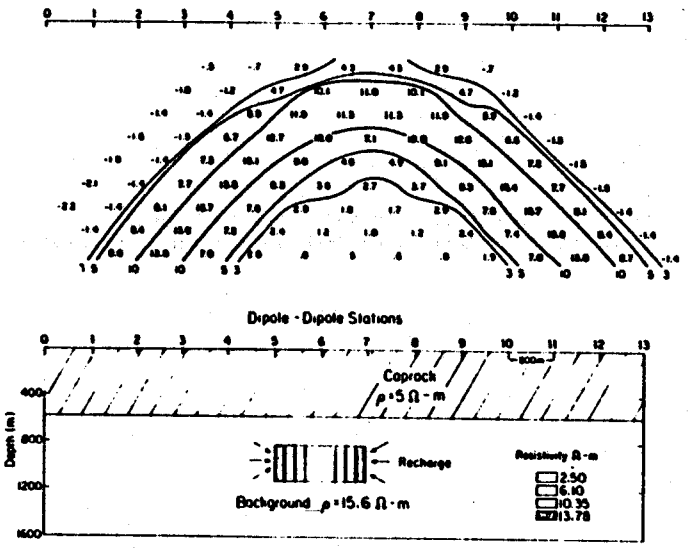

(b) 3 years

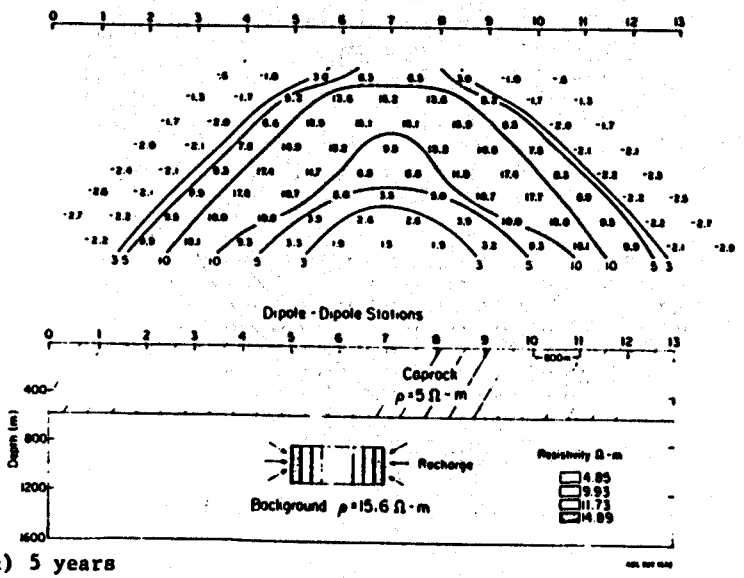

(c) 5 years

Figure 8. Dipole-dipole apparent resistivity pseudosections for reservoir with lateral recharge (percent changes).

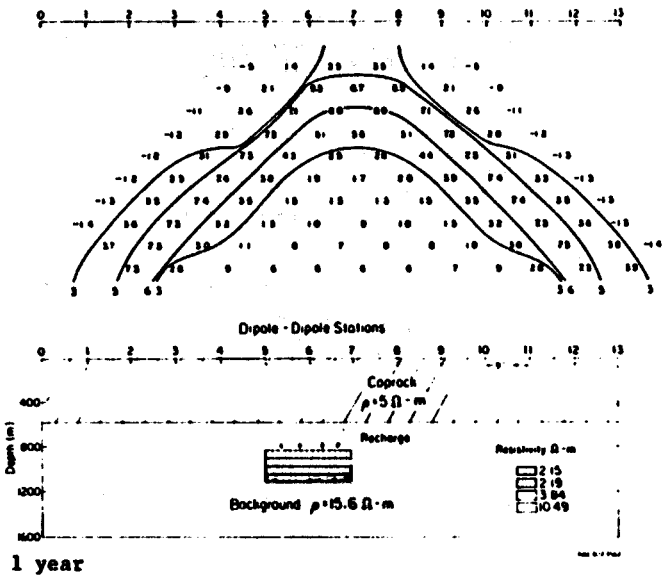

(a) 1 year

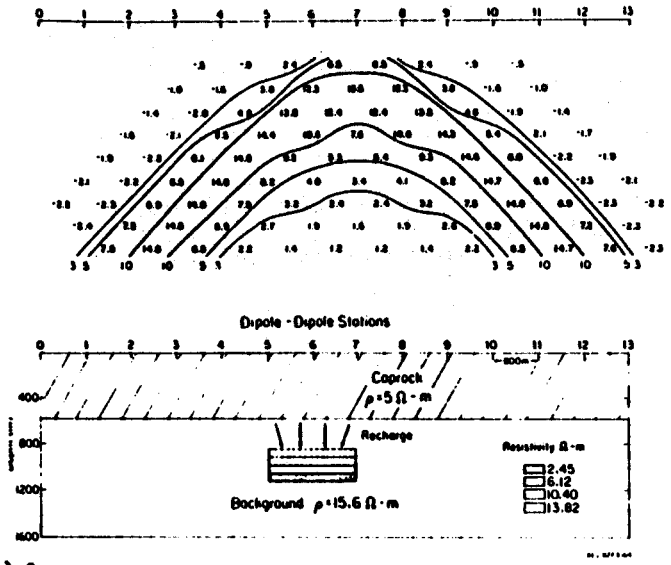

(b) 3 years

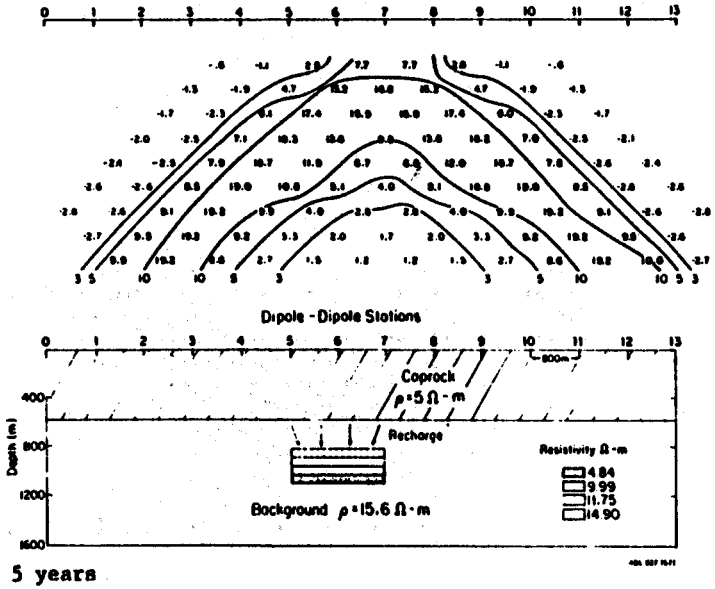

(c) 5 years

Figure 9. Resistivity pseudosections for reservoir with vertical recharge (percent changes).

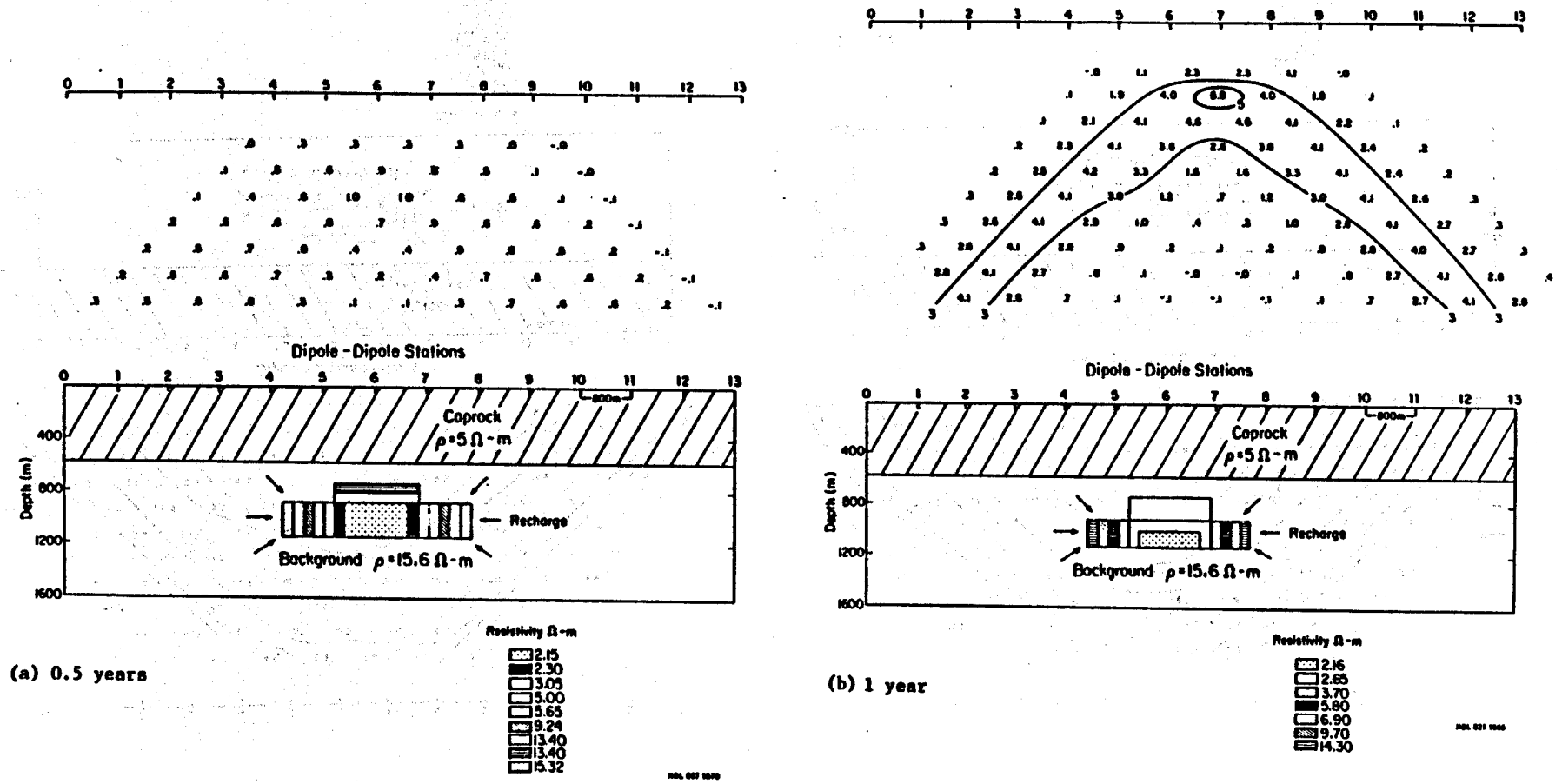

Figure 10. Resistivity pseudosections for reservoir with vertical and lateral recharge (percent changes).

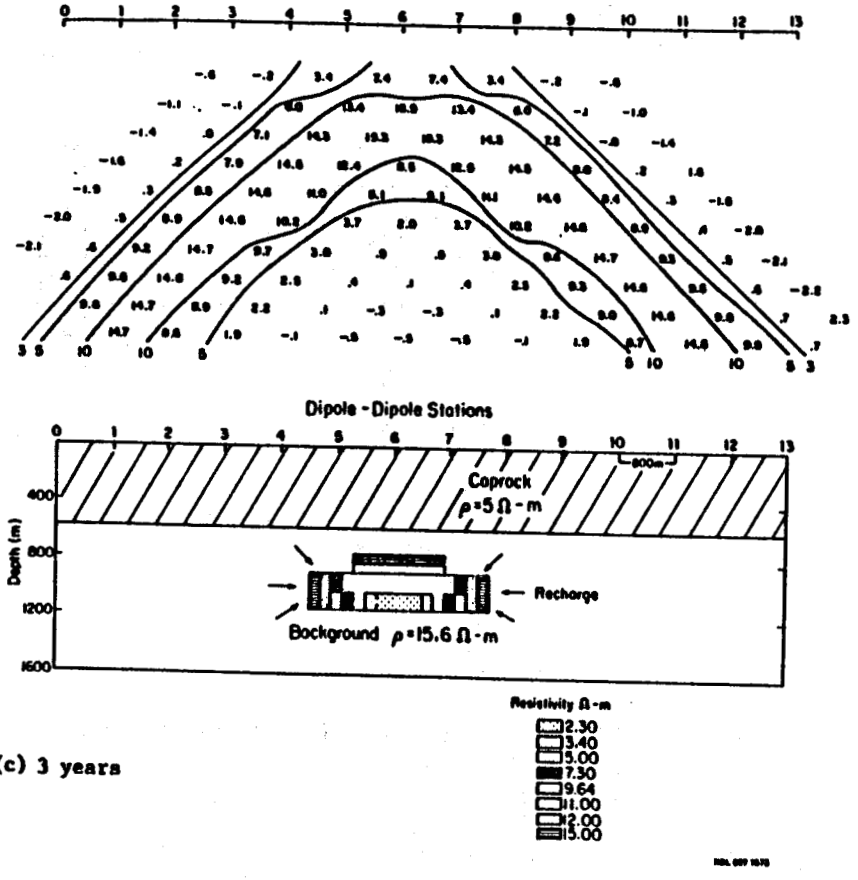

(c) 3 years

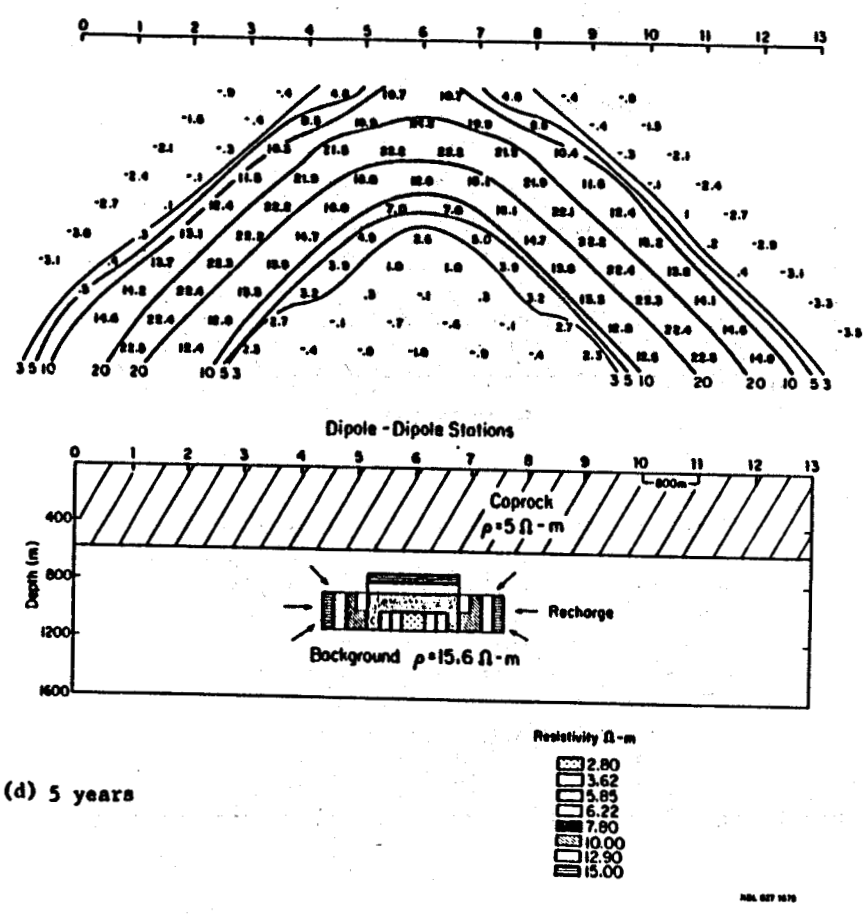

(d) 5 years

Figure 10 (continued).

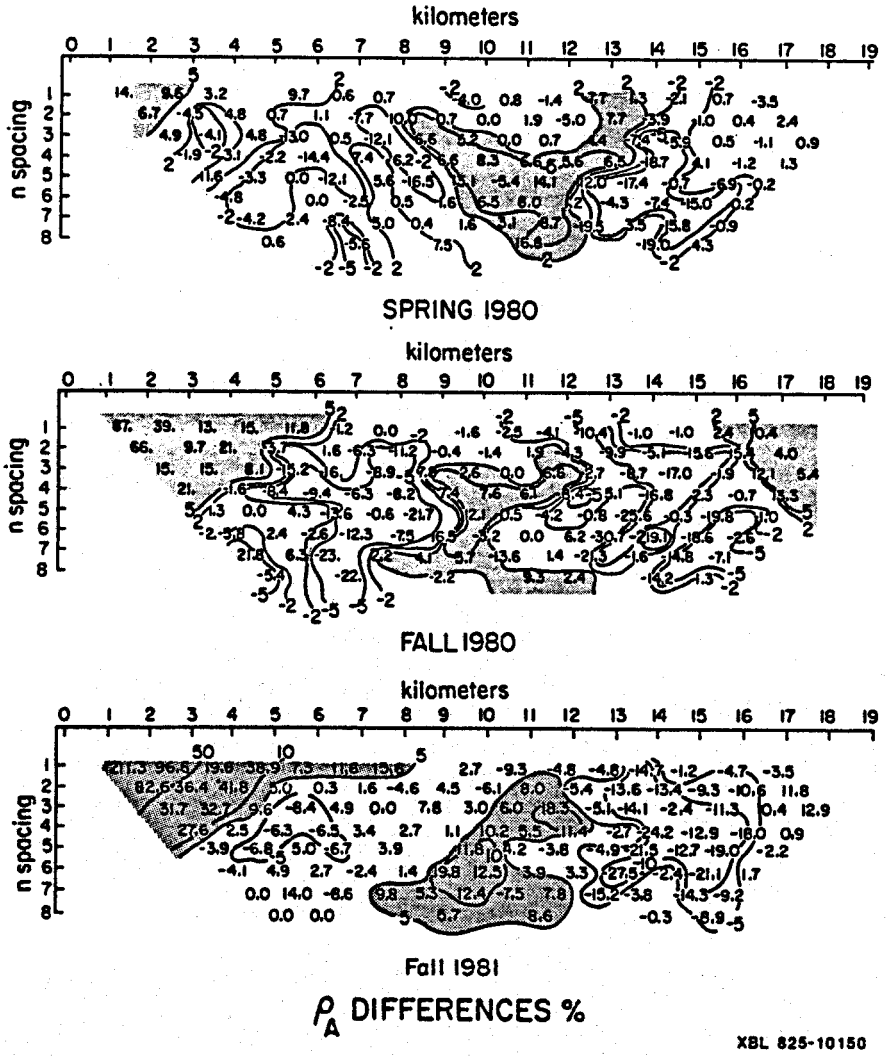

Figure 11. Resistivity pseudosections as measured in Cerro Prieto (percent changes from 1979 baseline).